

**Vacuum ultraviolet absorption spectra and photodissociative excitation of  $\text{CHBr}_2\text{Cl}$  and  $\text{CHBrCl}_2$**

Toshio Ibuki, Atsunari Hiraya, and Kosuke Shobatake

Citation: *The Journal of Chemical Physics* **96**, 8793 (1992); doi: 10.1063/1.462286

View online: <http://dx.doi.org/10.1063/1.462286>

View Table of Contents: <http://scitation.aip.org/content/aip/journal/jcp/96/12?ver=pdfcov>

Published by the [AIP Publishing](#)

---

**Articles you may be interested in**

[Photodissociative excitation processes of  \$\text{XeF}\_2\$  in the vacuum ultraviolet region 105–180 nm](#)

*J. Chem. Phys.* **102**, 5966 (1995); 10.1063/1.469331

[Vacuum ultraviolet absorption spectra of the bromomethanes](#)

*J. Chem. Phys.* **62**, 848 (1975); 10.1063/1.430535

[Vacuum ultraviolet absorption spectra of fluoromethanes](#)

*J. Chem. Phys.* **59**, 762 (1973); 10.1063/1.1680086

[Photodissociation of  \$\text{OCCl}\_2\$  in the Vacuum Ultraviolet: Production and Electronic Energy of Excited  \$\text{Cl}\_2\$](#)

*J. Chem. Phys.* **55**, 373 (1971); 10.1063/1.1675531

[Absorption Spectra of Some Organic Solutions in the Vacuum Ultraviolet](#)

*J. Chem. Phys.* **11**, 535 (1943); 10.1063/1.1723797

---



# Vacuum ultraviolet absorption spectra and photodissociative excitation of $\text{CHBr}_2\text{Cl}$ and $\text{CHBrCl}_2$

Toshio Ibuki

*Department of Chemistry, Kyoto University of Education, Fukakusa, Fushimi-ku, Kyoto 612, Japan*

Atsunari Hiraya and Kosuke Shobatake

*Institute for Molecular Science, Okazaki 444, Japan*

(Received 30 December 1991; accepted 11 March 1992)

Photoabsorption and fluorescence excitation spectra of  $\text{CHBr}_2\text{Cl}$  and  $\text{CHBrCl}_2$  trihalomethanes were measured in the 106–200 nm region using synchrotron radiation as a light source. Main photoabsorption bands observed are assigned as the Rydberg transitions of the outer shell orbitals. In the photoexcitation of  $\text{CHBr}_2\text{Cl}$  a diffuse emission band of  $\text{CHCl}(\tilde{A}^1A'' \rightarrow \tilde{X}^1A')$  was observed in the 500–800 nm region. The radiative lifetime of the  $\text{CHCl}(\tilde{A}^1A'')$  state was first determined to be  $7.01 \pm 0.25 \mu\text{s}$ . In the photolysis of  $\text{CHBrCl}_2$  at 121.6 nm, the formation of  $\text{CHCl}(\tilde{A}^1A'')$  and  $\text{CCl}_2(\tilde{A}^1B_1)$  radicals were observed. The fluorescence thresholds for  $\text{CHBr}_2\text{Cl}$  and  $\text{CHBrCl}_2$  start at 162 and 159 nm with the maximum yields of 5% and 11% at 122 and 119 nm, respectively.

## I. INTRODUCTION

Trihalomethanes typified by  $\text{CHBr}_2\text{Cl}$  and  $\text{CHBrCl}_2$  have been detected in drinking water and rivers as pollutants, and nowadays they pollute air too. This work is an extension of our earlier investigations of the vacuum ultraviolet (VUV) photoabsorption and fluorescence cross sections of halogenated methanes of  $\text{CCl}_4$ ,  $\text{CBrCl}_3$ ,<sup>1</sup>  $\text{CFCl}_3$ ,  $\text{CF}_2\text{Cl}_2$ ,<sup>2</sup>  $\text{CHFCl}_2$ , and  $\text{CHFBr}_2$ .<sup>3</sup> We have not found the previous photoabsorption measurements of  $\text{CHBr}_2\text{Cl}$  and  $\text{CHBrCl}_2$  molecules. Since atomic Cl plays an important role in atmospheric chemistry, it is of interest to measure the quantitative data of trihalomethanes in the VUV region.

In the present paper we report (i) the photoabsorption and fluorescence cross sections of  $\text{CHBr}_2\text{Cl}$  and  $\text{CHBrCl}_2$  in the 106–200 nm region, and (ii) the fluorescence spectral data of  $\text{CHCl}(\tilde{A}^1A'' \rightarrow \tilde{X}^1A')$  and  $\text{CCl}_2(\tilde{A}^1B_1 \rightarrow \tilde{X}^1A_1)$  transitions produced in the photodissociative excitation of the trihalomethanes. The Rydberg assignments will be discussed for the observed photoabsorption bands.

## II. EXPERIMENT

The experimental arrangement has been described in detail in previous papers.<sup>1–3</sup> In brief, synchrotron radiation produced from the 750 MeV electron storage ring at the Institute for Molecular Science (IMS) was dispersed by a 1 m Seya monochromator and introduced into a gas cell with LiF windows. The experimental uncertainty for the photoabsorption cross section is estimated to be better than 10% of the given value. The fluorescence excitation spectra were obtained using a cooled photomultiplier tube (PMT, Hamamatsu R955 sensitive 160–930 nm) settled in a direction perpendicular to the primary photon beam. The dispersed fluorescence and radiative lifetime were measured using H Lyman- $\alpha$  line (121.6 nm or 10.20 eV) generated by a 2.54 GHz microwave or dc discharge of  $\text{H}_2$ . The optical response to detect the dispersed fluorescence was corrected by a stan-

dard bromine lamp with a known spectral irradiance. The absolute fluorescence cross section was estimated by comparing the fluorescence intensity with the  $\text{OH}(A^2\Sigma^+ \rightarrow X^2\Pi)$  for which the fluorescence cross section has been known.<sup>4</sup>

Dibromochloro- and bromodichloromethanes were purchased from Nacalai Tesque Co. and purified by distillation in vacuum.

## III. RESULTS AND DISCUSSION

### A. $\text{CHBr}_2\text{Cl}$

The photoabsorption cross section of  $\text{CHBr}_2\text{Cl}$  in the 106–200 nm region is depicted by the solid curve in Fig. 1, which was measured with a resolution of 0.2 nm. There appear many photoabsorption bands. The electronic configuration of the outer shells of  $\text{CHBr}_2\text{Cl}$  can be expressed as

$$(3a'')^2(5a'')^2(4a'')^2(6a'')^2(5a'')^2(7a'')^2(6a'')^2 \quad (1)$$

by using photoelectron spectroscopy (PES) data,<sup>5</sup> in which the vertical ionization potentials (IP) from  $3a''$  to  $6a''$  have been determined to be in order 15.20, 12.33, 12.14, 11.61, 11.24, 11.06, and 10.69 eV, respectively. The outermost four molecular orbitals (MO) mainly represent the characteristics of the lone pair electrons of Br atoms ( $n_{\text{Br}}$ ), and the next outer  $6a'$  and  $4a''$  MO's are attributed to the  $n_{\text{Cl}}$  character.<sup>5</sup> The C–Br bonding electrons are expressed by  $3a''$  MO.

The band position for the lowest Rydberg transition of  $5s \leftarrow 6a''(n_{\text{Br}})$  is expected to appear around 170 nm using the empirical relation proposed by Robin:<sup>6</sup>

$$\chi_{\text{mol}} = \Sigma(n_i/N)(R/9N + Q_i), \quad (2)$$

where  $\chi_{\text{mol}}$  is the molecular term value, N is the total number of atoms in the molecule except hydrogen,  $n_i$  is the number of atoms in the molecule of the  $i$ th type, R is the Rydberg constant, and  $Q_i$  is a parameter depending on atom.  $Q_i$  values for C and Cl are 21 000 and  $\sim 25$  000  $\text{cm}^{-1}$ , respective-

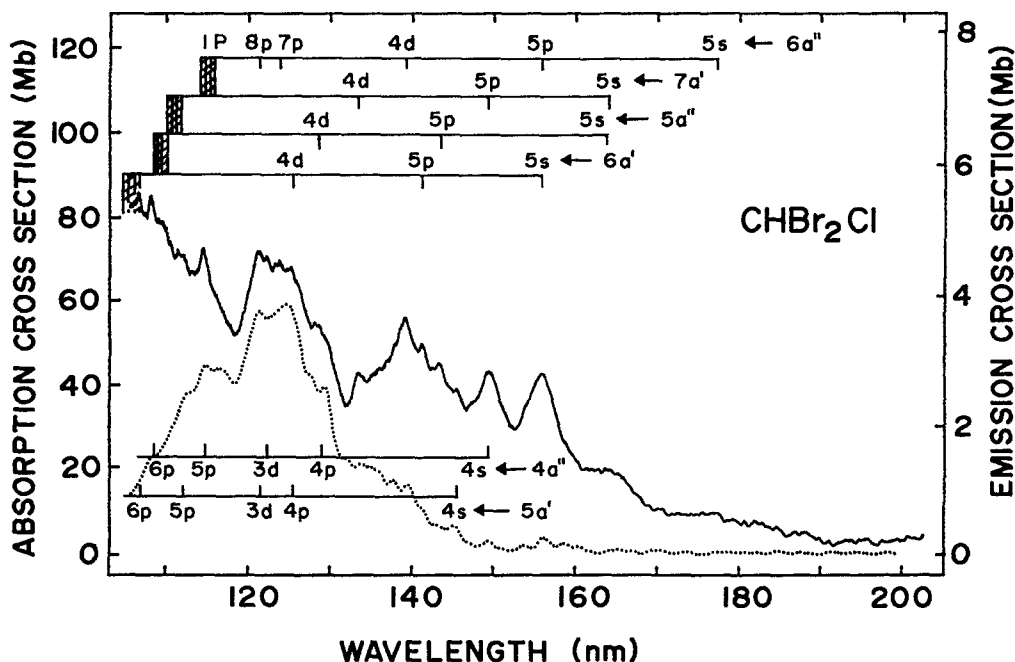


FIG. 1. Photoabsorption and fluorescence cross sections of  $\text{CHBr}_2\text{Cl}$  expressed by the solid and dotted curves, respectively. Spectral resolutions are 0.2 and 1.0 nm, respectively, for the photoabsorption and fluorescence excitation spectra where the photons emitted in the region 450–930 nm were detected.

ly,<sup>6</sup> and the  $Q_i$  value of Br atom is assumed to be the same with that of Cl given by Robin.<sup>6</sup>

The first weak, broad photoabsorption band peaked at  $178 \pm 3$  nm in Fig. 1 has the term value of  $30\,000 \pm 1000$   $\text{cm}^{-1}$  with respect to the lowest IP of 10.69 eV, and is close to  $\chi_{\text{mol}} = 27\,000$   $\text{cm}^{-1}$  calculated from Eq. (2). Therefore the weak band at around 178 nm can be assigned as the  $5s \leftarrow 6a''$  Rydberg transition with the quantum defect ( $\delta$ ) of 3.1 which is quite close to that for the  $5s \leftarrow 4p^2P^0$  Rydberg transitions of Br(I) atom with  $\delta = 3.06 \pm 0.07$ .<sup>7</sup> The photoabsorption band peaked at 155.8 nm, the uncertainty of which is estimated to be better than  $\pm 0.2$  nm, has the term values of 29 500 and 22 000  $\text{cm}^{-1}$  with respect to the IP's of  $6a'$  and  $6a''$ , respectively. The term value of 29 500  $\text{cm}^{-1}$  undoubtedly suggests the  $5s$ -terminating Rydberg excitation of  $6a'$  MO. Another  $\chi_{6a'}$  of 22 000  $\text{cm}^{-1}$  lies close to the term value of  $17\,800 \pm 2200$   $\text{cm}^{-1}$  for the  $5p \leftarrow 4p^2P^0$  Rydberg transitions of Br(I).<sup>7</sup> Thus, the band at 155.8 nm is superimposed by the  $5p \leftarrow 6a''$  and  $5s \leftarrow 6a'$  Rydberg transitions. Using the similar term value concepts, the absorption bands of  $\text{CHBr}_2\text{Cl}$  are assigned as the Rydberg type excitations of  $n_{\text{Br}}$  and  $n_{\text{Cl}}$  orbitals as listed in Table I. The averaged quantum defects of  $n_{\text{Br}}$  MO's to the  $5s$ ,  $np$ , and  $4d$  Rydberg levels are  $3.06 \pm 0.03$ ,  $2.72 \pm 0.09$ , and  $1.20 \pm 0.06$ , respectively (see Table I), which nicely fit with those of atomic Br:  $\delta = 3.06 \pm 0.07(5s)$ ,  $2.56 \pm 0.14(np)$ , and  $1.25 \pm 0.36(6d)$ .<sup>7</sup> In the  $n_{\text{Cl}}$  Rydberg excitation, the deduced quantum defects to the  $4s$ ,  $np$ , and  $3d$  levels are  $2.12 \pm 0.01$ ,  $1.66 \pm 0.05$ , and  $0.43 \pm 0.04$ , respectively.

TABLE I. Rydberg assignments for the photoabsorption bands of  $\text{CHBr}_2\text{Cl}$ .<sup>a</sup>

Band maximum (nm)	Assignment	Term value <sup>b</sup> ( $\text{cm}^{-1}$ )	$n^*$	$\delta$
178	$5s \leftarrow 6a''$	30 040	1.91	3.09
164	$5s \leftarrow 7a'$	28 200	1.97	3.03
	$5s \leftarrow 5a''$	29 700	1.92	3.08
155.8	$5p \leftarrow 6a''$	22 000	2.23	2.77
	$5s \leftarrow 6a'$	29 500	1.93	3.07
149.3	$5p \leftarrow 7a'$	22 200	2.22	2.78
	$4s \leftarrow 4a''$	30 900	1.88	2.12
145.4	$4s \leftarrow 5a'$	30 700	1.89	2.11
143.4	$5p \leftarrow 5a''$	20 900	2.29	2.71
141.2	$5p \leftarrow 6a'$	22 800	2.19	2.81
139.2	$4d \leftarrow 6a''$	14 400	2.76	1.24
133.5	$4d \leftarrow 7a'$	14 300	2.77	1.23
129.0	$4d \leftarrow 5a''$	13 100	2.89	1.11
	$4p \leftarrow 4a''$	20 400	2.32	1.68
125.5	$4d \leftarrow 6a'$	14 000	2.80	1.20
	$4p \leftarrow 5a'$	19 800	2.36	1.64
124.2	$7p \leftarrow 6a''$	5 700	4.39	2.61
122.5	$3d \leftarrow 4a''$	16 300	2.60	0.40
121.3	$8p \leftarrow 6a''$	3 780	5.39	2.61
	$3d \leftarrow 5a'$	17 000	2.54	0.46
114.2	$5p \leftarrow 4a''$	10 300	3.26	1.74
112.0	$5p \leftarrow 5a''$	10 200	3.29	1.71
108.4	$6p \leftarrow 4a''$	5 660	4.40	1.60
106.7	$6p \leftarrow 5a'$	5 730	4.38	1.62

<sup>a</sup>  $n^*$  is the effective principal quantum number and  $\delta$  is the quantum defect. The uncertainty of the peak is estimated to be better than  $\pm 0.2$  nm except the bands at 178 and 164 nm which have the uncertainty of  $\pm 3$  nm.

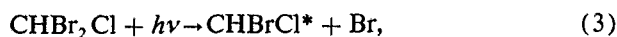
<sup>b</sup> See Ref. 5 for the ionization potentials.

They are also in excellent agreement with the  $\delta$  values for Cl atom of  $2.14 \pm 0.04(4s)$ ,  $1.63 \pm 0.12(np)$ , and  $0.40 \pm 0.13(4d)$ , respectively.<sup>7</sup> The  $\delta$  values for Cl atom are smaller than those for Br by  $\sim 1$  because Cl and Br lie in the third and fourth rows in the Periodic Table, respectively.

The photoabsorption shapes in Fig. 1 are indicative that the *s*- or *p*-terminating Rydberg transition gives a broad or sharp band feature, respectively, as widely observed in the group IV chlorides and bromides.<sup>1-3,8,9</sup>

The fluorescence excitation spectrum of  $\text{CHBr}_2\text{Cl}$  is shown by a dotted curve in Fig. 1 where photons in the region 450–930 nm were detected by using a sharp-cut filter. The absolute fluorescence cross section at 121.6 nm is deduced to be 3.7 Mb. The experimental uncertainty is estimated to be  $\pm 50\%$  since the OH fluorescence cross section has the uncertainty of  $\pm 36\%$ .<sup>4</sup> Additionally, the irradiance of the present standard lamp and the photon flux of the primary beam have  $\pm 5\%$  error. The emission intensity decreases strongly when the ionization channels open, suggesting that the cross section to produce ionic species becomes large at high photon energy.

Figure 2 shows the dispersed fluorescence observed in the photodissociative excitation of  $\text{CHBr}_2\text{Cl}$  at 121.6 nm. The spectral resolution is about 5 nm. The emission at 430 nm is apparently the  $\text{CH}(A^2\Delta \rightarrow X^2\Pi)$  transition produced through the following processes:



$$\Delta H = 10.4 \text{ eV},$$

where the weakest C–Br bond may be broken in the first step and the formation of  $\text{BrCl}^*$  molecule in the next step is considered to be improbable judging from the observation that no emitting halogen molecule has been observed in the previous photodissociative studies of halomethanes.<sup>1-3</sup> The threshold energy to generate  $\text{CH}(A^2\Delta)$  is calculated to be 10.4 eV using the heats of formation listed in Table II.<sup>10,11</sup> The calculated heat of reaction is slightly higher than the

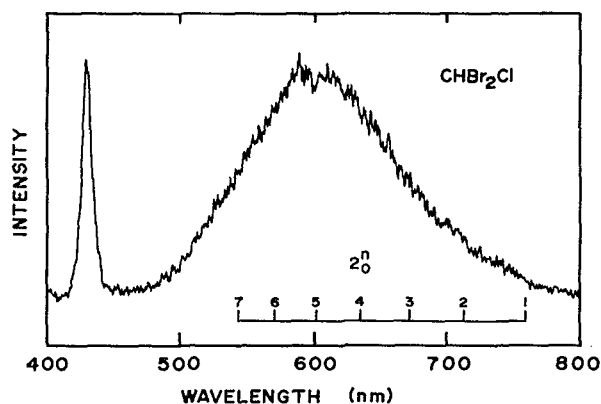


FIG. 2. Dispersed fluorescence spectrum observed in the photodissociative excitation of  $\text{CHBr}_2\text{Cl}$  at  $h\nu = 121.6$  nm. Sample pressure is 40 mTorr. Spectral resolution is about 5 nm.

TABLE II. Thermochemical data on  $\text{CHBr}_2\text{Cl}$  and  $\text{CHBrCl}_2$  decompositions.<sup>a</sup>

Species	$\Delta H_f^{298}$	Ref.
$\text{CHBr}_2\text{Cl}$	2.14 <sup>b</sup>	10
$\text{CHBrCl}_2$	-11.67 <sup>b</sup>	10
H	$52.100 \pm 0.001$	11
Cl	$28.922 \pm 2$	11
Br	26.740	11
BrCl	$3.50 \pm 0.3$	11
CH	$142.0 \pm 0.1$	11
CHCl	$80 \pm 10^b$	11
	$85.8 \pm 2$	Present work
$\text{CCl}_2$	$57 \pm 5$	11

<sup>a</sup> Units in kcal mol<sup>-1</sup>.

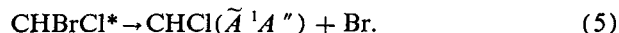
<sup>b</sup> Estimated value.

photon energy of 121.6 nm (10.20 eV), but we do not think the difference is serious since the heats of formation for  $\text{CHBr}_2\text{Cl}$  and  $\text{BrCl}$  are not determined experimentally but only estimated.<sup>10,11</sup>

We assign the structureless emission band spreading over 500–800 nm as the  $\text{CHCl}(\tilde{A}^1A'' \rightarrow \tilde{X}^1A')$  transition. Possible species to emit in the  $\text{CHBr}_2\text{Cl}$  photolysis are  $\text{Br}_2$ ,  $\text{CHCl}$ ,  $\text{CHBr}$ ,  $\text{CBr}_2$ ,  $\text{CBrCl}$ ,  $\text{CHXY}$  (X and Y are Br or Cl), and  $\text{CBr}_2\text{Cl}$  radicals in their electronically excited states. The lifetimes reported for the excited  $\text{Br}_2$ ,  $\text{CBr}_2$ , and  $\text{CBrCl}$  are far from that obtained in the present work as discussed in Sec. III B. We do not know of any previous studies of emission from  $\text{CHBr}$ ,  $\text{CHXY}$ , and  $\text{CBr}_2\text{Cl}$  radicals.

Photoabsorption bands of  $\text{CHCl}$  radical have been observed in the 550–820 nm region by Merer and Travis.<sup>12</sup> The  $\nu_2$  vibrational progression is indicated by bars in Fig. 2, and each  $\nu_2$  mode is accompanied by many rotational fine structures.<sup>12</sup> The band origin of  $\text{CHCl}(\tilde{A} \leftarrow \tilde{X})$  transition lies near 814 nm.<sup>12</sup> Some of the bands have also been found using gas phase laser induced fluorescence (LIF) by Kakimoto, Saito, and Hirota,<sup>13</sup> and Qiu, Zhou, and Shi.<sup>14</sup> The ground state of  $\text{CHCl}$  radical has a bent form with an equilibrium of  $105.1 \pm 4.7^\circ$ ,<sup>13</sup> and the electronically excited  $^1A''$  state, although bent, has a low barrier to linearity and is easily straightened by vibration.<sup>12</sup> The emission spectrum in Fig. 2 indicates that the electronic transition moments between the quasilinear and bent states of  $\text{CHCl}$  radical are large at  $\nu_2 = 4-6$  in the upper state. This observation consists with the LIF excitation spectrum of  $\text{CHCl}$  by Qiu *et al.*,<sup>14</sup> where the LIF signals at  $\nu_2 = 4$  and 5 have been observed much stronger than that at  $\nu_2 = 3$ .

The threshold wavelength for the  $\text{CHCl}(\tilde{A} \rightarrow \tilde{X})$  emission starts at  $162 \pm 1.5$  nm as shown in Fig. 1. The emission onset of  $176 \pm 2$  kcal/mol should be equal to the adiabatic heat of reaction for the  $\text{CHCl}(\tilde{A}^1A'')$  formation through the decomposition of  $\text{CHBrCl}^*$  radical produced by reaction (3):



Adopting the heats of formation given in Table II and the energy difference of 35.1 kcal/mol (814 nm) between the  $\tilde{A}^1A''$  and  $\tilde{X}^1A'$  states of  $\text{CHCl}$ ,<sup>12</sup> we deduce the heat of

formation of  $\Delta H_f(\text{CHCl}) = 85.8 \pm 2$  kcal/mol. This  $\Delta H_f$  value seems reasonable since a value of  $80 \pm 10$  kcal/mol has been estimated.<sup>11</sup>

A typical time dependent profile of the  $\text{CHCl}(\tilde{A}^1A'' \rightarrow \tilde{X}^1A')$  transition is depicted in Fig. 3 which was determined by a delayed coincidence–single photon counting technique. The decay curve is satisfactorily analyzed as a superposition of two components, which have also been observed in the cases of  $\text{CCl}_2(\tilde{A}^1B_1)$ ,<sup>1</sup>  $\text{CClF}(\tilde{A}^1A'')$ ,<sup>2</sup> and  $\text{CHF}(\tilde{A}^1A'')$  decays.<sup>3</sup> The Stern–Volmer plot of the fast decaying component shown in Fig. 4 gives the radiative lifetime of  $7.01 \pm 0.25 \mu\text{s}$  with the quenching rate constant of  $(4.12 \pm 0.07) \times 10^{-10} \text{ cm}^3/\text{molecule s}$ . These values are the first observation of the  $\text{CHCl}(\tilde{A}^1A'')$  state. The lifetime was determined by detecting the emission at two different wavelength regions: (i) 500–850 nm using a sharp-cut filter (Toshiba Y-50) and a PMT (Hamamatsu R649, sensitive 300–850 nm), and (ii) 630–850 nm with a R-63 filter. In the present experimental conditions there appears no discernible difference in the radiative lifetimes which may depend on the vibrational bands of  $\text{CHCl}(\tilde{A}^1A'')$  radical.

The radiative lifetime presently determined is different from those for  $\text{CBr}_2(\tilde{A})$  and  $\text{CBrCl}(\tilde{A})$  of 5.6 and 14.5  $\mu\text{s}$ , respectively.<sup>15</sup> The lifetimes for the  $A^3\Pi$  and  $B^3\Pi$  states of  $\text{Br}_2$  molecule have been estimated to be long: 1000–2000 and 12–70  $\mu\text{s}$ , respectively.<sup>16</sup> Thus, we assigned the present emitter to be  $\text{CHCl}(\tilde{A})$  radical as mentioned already.

## B. $\text{CHBrCl}_2$

Photoabsorption and fluorescence cross sections of  $\text{CHBrCl}_2$  in the 106–200 nm region are shown in Fig. 5 by the solid and dotted curves, respectively, where photons in the region 390–930 nm were detected in the fluorescence excitation spectrum. We adopt the similar term value concepts for the assignments of the photoabsorption bands. The outer shell orbitals of  $\text{CHBrCl}_2$  should be the same with the expression (1). The  $n_{\text{Br}}$  character is expressed by the outer-

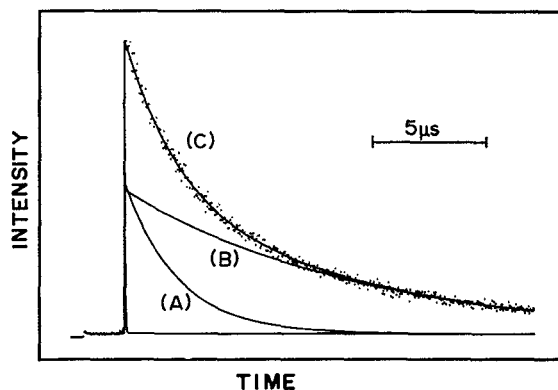


FIG. 3. A typical decay profile of the  $\text{CHCl}(\tilde{A}^1A'' \rightarrow \tilde{X}^1A')$  transition. Curves A and B are the fast and slowly decaying components, respectively. Curve C is the best fit convoluted result. The points indicate the experimental data.

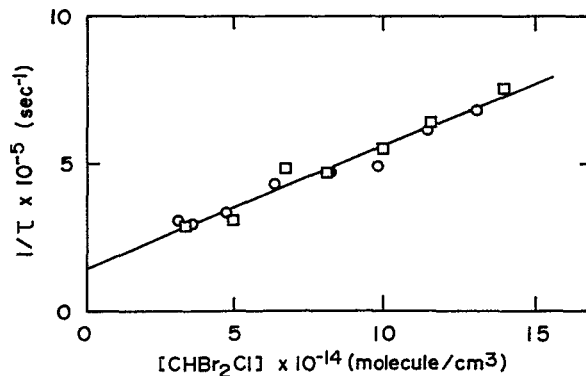


FIG. 4. Stern–Volmer plots of the fast decaying component.  $\square$ :  $\lambda_{\text{obs}} = 500\text{--}850$  nm,  $\circ$ : 630–850 nm.

most  $6a''$  and  $7a'$ , and the next four MO's are attributed to  $n_{\text{Cl}}$ .<sup>5</sup> The PES data have revealed the IP's in order 15.67, 12.55, 11.92, 11.71, 11.26, and 10.96 eV from  $3a''$  to  $6a''$ , respectively,<sup>5</sup> in which the IP's of  $5a'$  and  $4a''$  ( $n_{\text{Cl}}$ ) lie close and give rise to a single PES band at 12.55 eV.

The first weak band peaked at  $187 \pm 2$  nm has a large term value of  $35\,000 \text{ cm}^{-1}$  with respect to the lowest IP of 10.96 eV, and is assigned to be an allowed  $\sigma^* \leftarrow 6a''$  intravalent transition. The Rydberg assignments for other bands are listed in Table III. The deduced quantum defects for  $n_{\text{Br}}$  orbitals are  $3.00 \pm 0.06$ ,  $2.65 \pm 0.05$ , and  $1.41 \pm 0.10$  for the excitation to  $5s$ ,  $np$ , and  $4d$  Rydberg levels, respectively. In the Rydberg transitions of  $n_{\text{Cl}}$  MO's, they are  $2.05 \pm 0.04$ ,  $1.67 \pm 0.11$ , and  $0.43 \pm 0.03$  for the  $4s$ ,  $np$ , and  $3d$  terminations, respectively. The appropriateness of these  $\delta$ 's deduced was already discussed in the  $\text{CHBr}_2\text{Cl}$  section.

The absolute fluorescence cross section at 121.6 nm is 6.2 Mb and increases up to 8.6 Mb at 118.6 nm. After then the emission intensity decreases steeply at the ionization thresholds of  $(6a'')^{-1}$  and  $(7a')^{-1}$ .

Figure 6(a) shows the dispersed fluorescence observed in the photolysis of  $\text{CHBrCl}_2$  at 121.6 nm. No structure is found with a low resolution of  $\sim 5$  nm. The spectral features at 400–500 nm region resemble those of  $\text{CCl}_2(\tilde{A}^1B_1 \rightarrow \tilde{X}^1A_1)$  spectrum shown by a solid curve in Fig. 6(b), which was measured in the decomposition of  $\text{CCl}_4$  at H Lyman- $\alpha$  line.<sup>1</sup> The difference emission intensity between the  $\text{CHBrCl}_2$  [Fig. 6(a)] and  $\text{CCl}_4$  [Fig. 6(b)] photoexcitations is depicted by lozenges in Fig. 6(b). The global features of this difference spectrum resemble closely those of  $\text{CHCl}(\tilde{A}^1A'' \rightarrow \tilde{X}^1A')$  transition shown in Fig. 2.

The radiative lifetime of the emitter in Fig. 6(a) was determined to be  $1.77 \pm 0.15 \mu\text{s}$  by detecting photons at  $\lambda_{\text{obs}} = 457 \pm 6.8$  nm by inserting an interference filter (Toshiba KL-46) in front of the PMT to detect the fluorescence profile. This lifetime is close to the previous value of  $2.17 \pm 0.26$  (Ref. 1) or  $1.83 \pm 0.02 \mu\text{s}$  for  $\text{CCl}_2(\tilde{A}^1B_1 \rightarrow \tilde{X}^1A_1)$  transition.<sup>17</sup> Another radiative lifetime of  $6.80 \pm 0.30 \mu\text{s}$  was obtained by detecting photons at the 630–850 nm region, in which the contribution of the  $\text{CCl}_2(\tilde{A}^1B_1)$  emission is considered to be minor (see Fig.

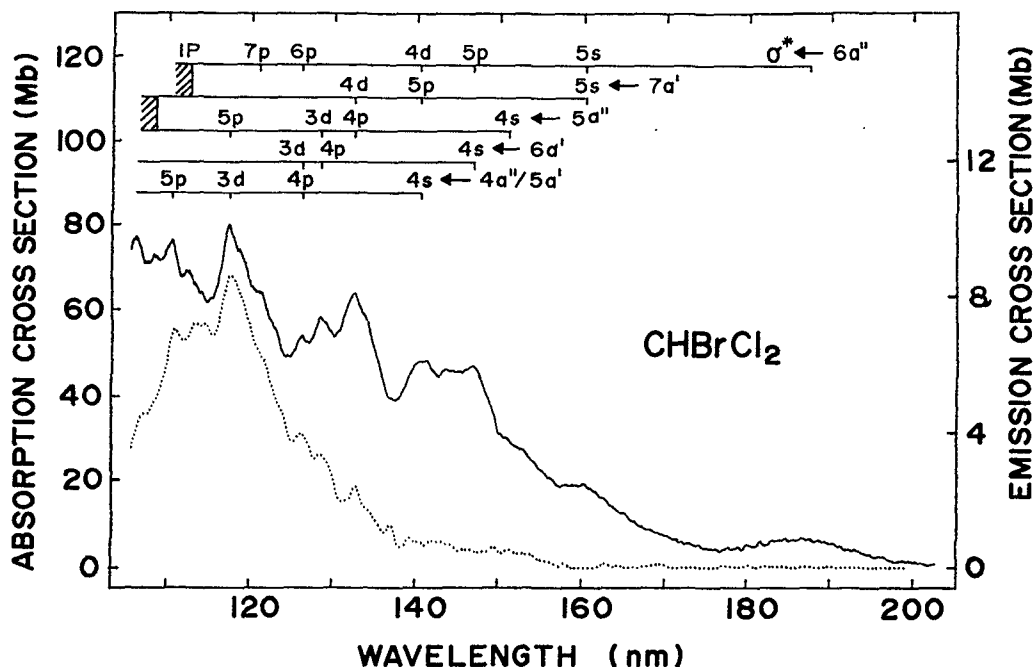


FIG. 5. Photoabsorption and fluorescence cross sections of  $\text{CHBrCl}_2$ , expressed by the solid and dotted curves, respectively. Spectral resolutions are the same as those in Fig. 1. Photons in the region 390–930 nm were detected in the fluorescence excitation measurement.

6). This lifetime at  $\lambda_{\text{obs}} = 630\text{--}850\text{ nm}$  is quite close to that of  $\text{CHCl}(\tilde{A}^1A'')$  state found in the  $\text{CHBr}_2\text{Cl}$  section, i.e.,  $7.01 \pm 0.25\ \mu\text{s}$ .

Judging from the above observations, we assign the emitters produced in the photodissociative excitation of

$\text{CHBrCl}_2$  are  $\text{CCl}_2(\tilde{A}^1B_1)$  and  $\text{CHCl}(\tilde{A}^1A'')$  radicals which may be formed through the following two steps similar to the production of  $\text{CHCl}(\tilde{A}^1A'')$ :

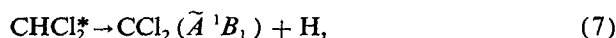
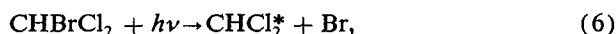


TABLE III. Rydberg assignments for the photoabsorption bands of  $\text{CHBrCl}_2$ .<sup>a</sup>

Band maximum (nm)	Assignment	Term value ( $\text{cm}^{-1}$ )	$n^*$	$\delta$
187	$\sigma^* - 6a''$	34 900		
160	$5s - 6a''$	26 000	2.05	2.95
	$5s - 7a'$	28 400	1.96	3.04
151	$4s - 5a''$	28 400	1.97	2.03
147	$5p - 6a''$	20 400	2.32	2.68
	$4s - 6a'$	28 100	1.98	2.02
141	$4d - 6a''$	17 300	2.52	1.48
	$5p - 7a'$	19 700	2.36	2.64
	$4s - 4a''/5a'$	30 100	1.91	2.09
132.8	$4d - 7a'$	15 500	2.66	1.34
	$4p - 5a''$	19 200	2.39	1.61
128.7	$3d - 5a''$	16 800	2.56	0.44
	$4p - 6a'$	18 400	2.44	1.56
126.4	$6p - 6a''$	9 300	3.44	2.56
	$3d - 6a'$	17 000	2.54	0.46
	$4p - 4a''/5a'$	22 100	2.23	1.77
121.2	$7p - 6a''$	5 890	4.32	2.68
117.7	$7p - 7a'$	5 860	4.33	2.67
	$5p - 5a''$	9 500	3.40	1.60
	$3d - 4a''/5a'$	16 300	2.60	0.40
110.5	$5p - 4a''/5a'$	10 700	3.20	1.80

<sup>a</sup> The uncertainty of the peak is estimated to be better than  $\pm 0.2\text{ nm}$  except the first five bands from 187 to 141 nm which have the uncertainty of  $\pm 2\text{ nm}$ .

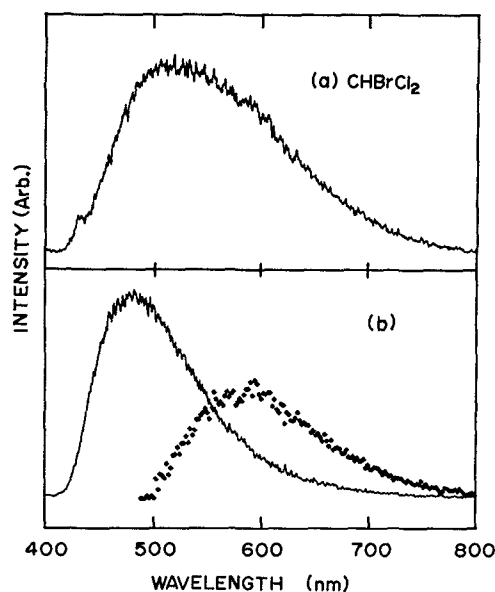
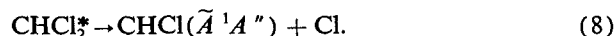


FIG. 6. (a) Dispersed fluorescence spectra observed in the photodissociative excitation of  $\text{CHBrCl}_2$  at  $h\nu = 121.6\text{ nm}$ . (b) Solid curve is the  $\text{CCl}_2(\tilde{A}^1B_1 \rightarrow \tilde{X}^1A_1)$  transition taken from Ref. 1. The lozenges indicate the "difference spectrum" showing the  $\text{CHCl}(\tilde{A}^1A'' \rightarrow \tilde{X}^1A')$  transition (see the text).



The threshold wavelengths to generate  $\text{CCl}_2(\tilde{A})$  and  $\text{CHCl}(\tilde{A})$  states through reactions (7) and (8) are calculated to be 146 and 152 nm, respectively, using the energy gap of 2.10 eV between the  $\tilde{A}^1B_1$  and  $\tilde{X}^1A_1$  states of  $\text{CCl}_2$ .<sup>18,19</sup> These onsets nicely fit to the emission threshold of  $159 \pm 1$  nm found in the fluorescence excitation spectrum in Fig. 5.

The fluorescence excitation spectra shown in Figs. 1 and 5 have some common features: Down to  $\lambda_{\text{exc}} \approx 140$  nm the emission intensity is weak, while the emission at around 120 nm is quite strong. In addition, these emission bands do not seem that they directly have any correlation with the Rydberg states discussed above. Especially the strong absorption bands assigned as the  $np$  and/or  $nd$  Rydberg levels at around 140 nm correspond to the position of the very weak emission intensity. Therefore, we suppose that the potential curves to form the emitters are not strongly correlated with the Rydberg levels but mainly with the intravalent excited states concealed in the photoabsorption spectra.

#### ACKNOWLEDGMENTS

The authors are grateful to the staff of the Ultraviolet Synchrotron Orbital Radiation (UVSOR) facility at IMS. This work was supported in part by the UVSOR joint research program.

- <sup>1</sup>T. Ibuki, N. Takahashi, A. Hiraya, and K. Shobatake, *J. Chem. Phys.* **85**, 5717 (1986).
- <sup>2</sup>T. Ibuki, A. Hiraya, and K. Shobatake, *J. Chem. Phys.* **90**, 6290 (1989).
- <sup>3</sup>T. Ibuki, A. Hiraya, K. Shobatake, Y. Matsumi, and M. Kawasaki, *J. Chem. Phys.* **92**, 4277 (1990).
- <sup>4</sup>L. C. Lee, *J. Chem. Phys.* **72**, 4334 (1980).
- <sup>5</sup>I. Novak, T. Cvitas, L. Klansinc, and H. Güsten, *J. Chem. Soc. Faraday Trans. 2* **77**, 2049 (1981).
- <sup>6</sup>M. B. Robin, *Higher Excited States of Polyatomic Molecules* (Academic, New York, 1974), Vol. 1.
- <sup>7</sup>C. E. Moore, *Atomic Energy Levels*, Nat. Stand. Ref. Data Ser. 35 (Nat. Bur. Stand., U. S. GPO, Washington, DC, Reissued 1971), Vol. 2.
- <sup>8</sup>G. C. Causley and B. R. Russell, *J. Electron Spectrosc. Relat. Phenom.* **8**, 71 (1976); **11**, 383 (1977).
- <sup>9</sup>J. B. Clark and B. R. Russell, *J. Electron Spectrosc. Relat. Phenom.* **11**, 371 (1977).
- <sup>10</sup>S. A. Kudchadker, and A. P. Kudchadker, *J. Chem. Phys. Res. Data* **7**, 1285 (1978).
- <sup>11</sup>D. R. Stull and H. Prophet, Project Editors, *JANAF Thermochemical Tables*, 2nd ed., Nat. Stand. Ref. Data Ser. 37 (Nat. Bur. Stand., U. S. GPO, Washington, DC, 1971).
- <sup>12</sup>J. A. Merer and D. N. Travis, *Can. J. Phys.* **44**, 525 (1966).
- <sup>13</sup>M. Kakimoto, S. Saito, and E. Hirota, *J. Mol. Spectrosc.* **97**, 194 (1983).
- <sup>14</sup>Y. Qiu, S. Zhou, and J. Shi, *Chem. Phys. Lett.* **136**, 93 (1987).
- <sup>15</sup>V. E. Bondybey and J. H. English, *J. Mol. Spectrosc.* **79**, 416 (1980).
- <sup>16</sup>K. P. Huber and G. Herzberg, *Molecular Spectra and Molecular Structure*, Vol. 4 (Van Nostrand, New York, 1979).
- <sup>17</sup>T. Ibuki, A. Hiraya, and K. Shobatake, *Chem. Phys. Lett.* **157**, 521 (1989).
- <sup>18</sup>V. E. Bondybey, *J. Mol. Spectrosc.* **64**, 180 (1977).
- <sup>19</sup>D. A. Predmore, A. M. Murray, and M. D. Harmony, *Chem. Phys. Lett.* **110**, 173 (1984).